Colloidal PbS and PbSeS Quantum Dot Sensitized Solar Cells Prepared by Electrophoretic Deposition

ARTICLE *in* THE JOURNAL OF PHYSICAL CHEMISTRY C · JULY 2012

Impact Factor: 4.77 · DOI: 10.1021/jp3056009

7 AUTHORS, INCLUDING:

Nima Parsi Benehkohal
McGill University
10 PUBLICATIONS **71** CITATIONS
SEE PROFILE

Sudam Chavhan
IK4-CIDETEC
26 PUBLICATIONS **487** CITATIONS
SEE PROFILE

Ramon Tena-Zaera
IK4-CIDETEC
73 PUBLICATIONS **2,415** CITATIONS
SEE PROFILE

Iván Mora-Seró
Universitat Jaume I
129 PUBLICATIONS **7,868** CITATIONS
SEE PROFILE

THE JOURNAL OF PHYSICAL CHEMISTRY C

Article

pubs.acs.org/JPCC

Colloidal PbS and PbSeS Quantum Dot Sensitized Solar Cells Prepared by Electrophoretic Deposition

Nima Parsi Benehkohal,*[,†] Victoria González-Pedro,[‡] Pablo P. Boix,[‡] Sudam Chavhan,[§] Ramón Tena-Zaera,[§] George P. Demopoulos,[†] and Iván Mora-Seró*[,‡]

[†]Department of Materials Engineering, McGill University, Montreal, Quebec H3A 2B2, Canada

[‡]Photovoltaic and Optoelectronic Devices Group, Departament de Física, Universitat Jaume I, 12071 Castelló de la Plana, Spain

[§]Energy Department, IK4-CIDETEC, Parque Tecnológico, Paseo Miramón 196, 20009 Donostia-San Sebastián, Spain

Supporting Information

ABSTRACT: Here we report the development of quantum dot sensitized solar cells (QDSCs) using colloidal PbS and PbSeS quantum dots (QDs) and polysulfide electrolyte for high photocurrents. QDSCs have been prepared in a novel sensitizing way employing electrophoretic deposition (EPD) and protecting the colloidal QDs from corrosive electrolyte with a CdS coating. EPD allows a rapid, uniform, and effective sensitization with QDs, while the CdS coating stabilizes the electrode. The effect of electrophoretic deposition time and of colloidal QD size on cell efficiency is analyzed. Efficiencies as high as 2.1 ± 0.2% are reported.

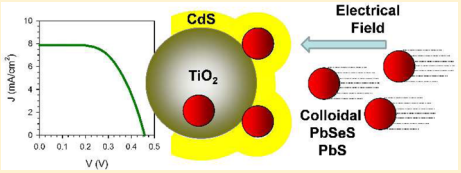

INTRODUCTION

The development of third-generation solar cells overcoming the Shockley−Queisser efficiency limit for a single absorber, 31%,[1] is one of the most fascinating challenges in the energy research field. In this aspect, semiconductor quantum dots (QDs) have shown extremely attractive properties for the development of solar cells overcoming the current limitations.[2] The demonstration of an efficient multiple exciton generation (MEG) process in colloidal QDs,[3,4] despite certain controversy,[5] has aroused a huge interest in the use of these materials in photovoltaic devices. This interest has been reinforced with the recent reports of absorbed photon-to-current efficiency (APCE) close to 200%[6] and incident photon-to-current efficiency (IPCE) as high as 114%.[7] These achievements are acquired by using QDs with IR absorption, PbS[6] and PbSe.[7] In the former case PbS QDs have been employed in a sensitized solar cell configuration.[8] Electron−hole pairs, photogenerated and produced by impact ionization in an MEG process, in PbS colloidal QDs are quickly separated into two different media. Electrons are injected into flat TiO_2 single crystals, while holes are regenerated by a polysulfide electrolyte.[6] Nanostructured TiO_2 electrodes, instead of flat electrodes, enhance dramatically light harvesting, but two main problems have to be solved: (i) uniform sensitization with colloidal QDs of a nanostructured electrode along all its thickness and (ii) development of a stable QDSC configuration with colloidal PbS QDs as sensitizers. We have addressed these problems preparing colloidal PbS and PbSeS quantum dot sensitized solar cells (QDSCs) in a novel sensitizing way employing electrophoretic deposition (EPD) and protecting the colloidal QDs from corrosive electrolytes with a CdS coating. We have analyzed the effect of electrophoretic deposition time and QD size in the final solar cell performance, obtaining efficiencies as high as 2.1 ± 0.2%. These results represent a significant advance in the development of colloidal QDSCs with light absorption in the IR region. In addition, we discuss the role of QDs in the recombination process of the analyzed solar cells.

Electrophoretic deposition has been used for the deposition of TiO_2 nanoparticles in solar cell[9] or photocatalytic[10] applications. In addition, it is a method also employed to deposit colloidal QDs, especially CdSe, on different materials such as Au,[11,12] patterned electrodes,[13] stacked-cup carbon nanotubes,[14] and polymer templates.[15] Colloidal CdSe QDs have also been deposited by electrophoresis for photovoltaic purposes. Electrophoretic deposition of CdSe-C60 was used for the preparation of composite films for solar energy generation.[16] Flexible QDSCs have been fabricated by using the electrophoretic deposition of CdSe QDs on ZnO nanorods, obtaining efficiencies of 0.98%.[17] Higher efficiencies, 1.7%, have been reported for TiO_2 nanostructured electrodes with a ZnS coating of the colloidal CdSe QDs,[18] but there is no report on the use of EPD of PbS or PbSeS QDs. Electrophoretic deposition presents a significant advantage over other deposition techniques for colloidal QDs, either as linker-assisted[19−21] or directly adsorbed,[19,21] because of its simplicity and short deposition time. While for electrophoretic deposition times as short as 2 h were sufficient for effective coating,[18] several hours or even days are needed with other techniques.[19−21]

The use of PbS QDs in QDSCs has been significantly less than the utilization of CdSe QDs, in spite of the higher light harvesting potential of PbS QDs due to their tunable

Received: June 7, 2012
Revised: July 12, 2012
Published: July 13, 2012

   dx.doi.org/10.1021/jp3056009 | J. Phys. Chem. C 2012, 116, 16391−16397

absorption in the IR range. This is largely due to the difficulty of finding an appropriate electrolyte for PbS in which it is stable. PbS is not stable with iodine nor polysulfide redox electrolytes.[22−24] Thus, most of the reports on PbS QDSCs are for all-solid devices.[23,25−27] In the case of using a liquid electrolyte for hole transport in PbS QDSCs, the highest reported efficiency, 0.62%, has been reported using a Co redox electrolyte,[28] at 1 sun, and with PbS grown by the successive ionic layer absorption and reaction (SILAR) method. We have shown that, by employing the same deposition technique, stable QDSCs using polysulfide electrolyte can be obtained by coating the PbS QDs with CdS,[29] reporting a significant efficiency of 2.36% using nanostructured TiO_2 electrodes.[30] Similar efficiencies have been obtained using SnO_2 electrodes,[31] and outstanding efficiencies of 3.82% have been obtained using TiO_2 photoanodes with hierarchical pore distribution,[32] employing again in both cases the SILAR growth. However, the presynthesis of colloidal QDs allows the preparation of QDs with better defined properties than QD samples prepared by SILAR. Treatment of colloidal PbS/TiO_2 cells using CdS grown by the SILAR method has been successfully applied before in a depleted heterojunction solar cell configuration.[33] The ultrafast electron injection from PbS colloidal QDs into TiO_2 as fast as 6.4 fs[34] points to the capability of extraction of charge generated by MEG. Thus, the preparation of cells with colloidal QDs is extremely interesting.

EXPERIMENTAL SECTION

Colloidal QDs. PbSSe QDs with oleic acid capping were kindly provided by NANOCO, while PbS QDs were purchased from Evident Technologies. Both QDs were solved in toluene.

Table 1. Solar Cell Parameters of QDSCs Prepared Employing PbSeS 800 nm QDs and Different Electrophoresis Deposition Times:[a] Open Circuit Voltage, V_{oc}, Short Circuit Current, J_{sc}, Fill Factor, FF, and Photovoltaic Conversion Efficiency, η

	V_{oc} (V)	J_{sc} (mA/cm^2)	FF	η (%)
5CdS	0.46	3.7	0.62	1.07
5 min	0.46 ± 0.04	4.3 ± 0.5	0.58 ± 0.03	1.14 ± 0.14
15 min	0.440 ± 0.15	5 ± 1	0.56 ± 0.01	1.1 ± 0.3
30 min	0.42 ± 0.2	5.6 ± 0.6	0.593 ± 0.005	1.4 ± 0.2
60 min	0.41 ± 0.2	6.14 ± 0.5	0.63 ± 0.01	1.58 ± 0.16
90 min	0.37	6.2	0.60	1.36

[a]5CdS is a sample prepared with no PbSeS QDs and just five SILAR cycles of CdS and two SILAR cycles of ZnS. The rest of the samples are identified by the PbSeS electrophoresis deposition time; in addition, all these samples have also been coated with five SILAR cycles of CdS and two SILAR cycles of ZnS.

TiO_2 Photoanode Preparation. After the fluorine-doped tin oxide (FTO) glasses (Pilkington TEC 8 with 8 Ω^2 sheet resistance) were cleaned, a compact layer of TiO_2 was deposited on them by spray pyrolysis of titanium(IV) bis(acetoacetonato) bis(isopropanoxylate) followed by sintering at 450 °C to improve the electrical contact between the nanoparticles. TiO_2 photoanodes were prepared by "double-layer" screen-printing on FTO glass using two different TiO_2 pastes, including a light-scattering layer on top of the transparent TiO_2 film. The transparent layer is formed by 20 nm TiO_2 nanoparticles (18NR-AO, Dyesol), and the opaque layer contains 300−400 nm TiO_2 particles (WER4-O Dyesol). Finally, the resulting film was sintered again at 450 °C for 30 min. The total thickness of the photoanodes was 15 ± 1 μm, measured with a Dektack 6 profilometer from Veeco.

Electrophoretic Deposition of the QDs on the TiO_2 Electrodes. QDs were diluted in toluene, with concentrations of ∼2.2 × 10^{-6} M. Two TiO_2 FTO electrodes were immersed vertically in the QD solution parallel to each other. The deposition area of the electrodes was about 0.25 cm^2, and the distance between them was adjusted at 1 cm. A voltage of 200 V was applied for 5−90 min. QDs were deposited on both the cathode and anode electrodes similar to previous reports.[18] Fresh layers at each deposition time were taken from the electrophoretic cell, rinsed several times with toluene to wash off unbound QDs, subsequently rinsed with ethanol, and dried at room temperature. After electrophoretic deposition colloidal QDs were coated with a CdS layer grown by SILAR. The SILAR process was carried out following the method recently described. Cd^{2+} ions were deposited from an ethanolic 0.05 M solution of $Cd(NO_3)_2{\cdot}4H_2O$. The sulfide source was a 0.05 M solution of $Na_2S{\cdot}9\ H_2O$ in methanol/water (50/50, v/v). A single SILAR cycle consisted of 1 min of dip-coating of the TiO_2 working electrode into the metal precursors and subsequent rinsing for 1 min in ethanol. Subsequently, the sample was dipped into the sulfide solution for 1 min and rinsed in methanol/water (50/50, v/v) for an additional 1 min. This procedure constitutes a complete SILAR cycle. The SILAR process was carried out automatically using a robot designed by ISTest. All the analyzed cells in this work were coated with ZnS, by being alternately dipped into 0.1 M $Zn(CH_3COO)_2$ and 0.1 M Na_2S Milli-Q water solutions for 1 min/dip and subsequently rinsed with Milli-Q ultrapure water. Two SILAR cycles were employed for ZnS coating.

QDSC Preparation. Porous Cu_2S was used as a counter electrode, which was prepared by immersing brass in HCl solution at 70 °C for 5 min and subsequently dipping it into polysulfide solution for 10 min.[19] The counter electrode and a QD-sensitized electrode were assembled into a sandwich-type configuration using a Scotch spacer (thickness 50 μm) and with a droplet (10 μL) of polysulfide electrolyte. The polysulfide electrolyte was composed of 1 M Na_2S, 1 M S, and 0.1 M NaOH solution in Milli-Q ultrapure water.

Photoanode and Solar Cell Characterization. The cross section morphology of the TiO_2−PbSeS electrode films was investigated using a field emission scanning electron microscope (ULTRA plus ZEISS FESEM). Energy-dispersive X-ray spectroscopy (Apollo X, Ametek EDAX) was employed to map and determine the distribution of chemical elements. A Bruker AXS-D8 Advance X-ray diffractometer, using Cu Kα radiation, was used to analyze the structural properties of anodes before and after light sensitization. The optical absorption spectra of the photoanodes were recorded at 300−700 nm using a Cary 500 UV−vis Varian photospectroscometer. The IPCE measurements were done using a 150 W Xe lamp coupled with a monochromator controlled by a computer; the photocurrent was measured using a 70310 optical power meter from Oriel Instruments, using a Si photodiode to calibrate the system. QDSCs were characterized by current−voltage and impedance spectroscopy using a 0.1256 cm^2 mask and no antireflective layer. These measurements were performed employing the PG-STAT30 potentiostat (Autolab) and solar simulator at AM1.5 G, where the light intensity was adjusted with an NREL calibrated Si solar cell with a KG-5 filter to 1 sun intensity (100 mW/cm^2). For most of the conditions analyzed in this work

dx.doi.org/10.1021/jp3056009 | J. Phys. Chem. C 2012, 116, 16391−16397

Table 2. Solar Cell Parameters of QDSCs Prepared Employing QDs of Different Types and Sizes:[a] Open Circuit Voltage, V_{oc}, Short Circuit Current, J_{sc}, Fill Factor, FF, and Photovoltaic Conversion Efficiency, η

	V_{oc} (V)	J_{sc} (mA/cm^2)	FF	η (%)
PbS 743 nm	0.425 ± 0.15	7.3 ± 0.7	0.61 ± 0.03	1.9 ± 0.2
PbSeS 800 nm	0.41 ± 0.2	6.14 ± 0.5	0.63 ± 0.01	1.58 ± 0.16
PbSeS 850 nm	0.39	6.4	0.49	1.2
PbS 1049 nm	0.322 ± 0.015	3.6 ± 0.8	0.584 ± 0.014	0.67 ± 0.14
PbS 1427 nm	0.234 ± 0.010	1.09 ± 0.12	0.46 ± 0.02	0.1235 ± 0.0003
PbS 743 nm, 9CdS	0.46 ± 0.07	8 ± 2	0.58 ± 0.03	2.1 ± 0.2
9CdS	0.515	5.79	0.60	1.8

[a]All the samples present the same electrophoresis deposition time, 60 min, and CdS/ZnS coating, five and two SILAR cycles, respectively, except the last one with nine and two SILAR cycles. A sample prepared just with nine SILAR cycles of CdS is included for comparison.

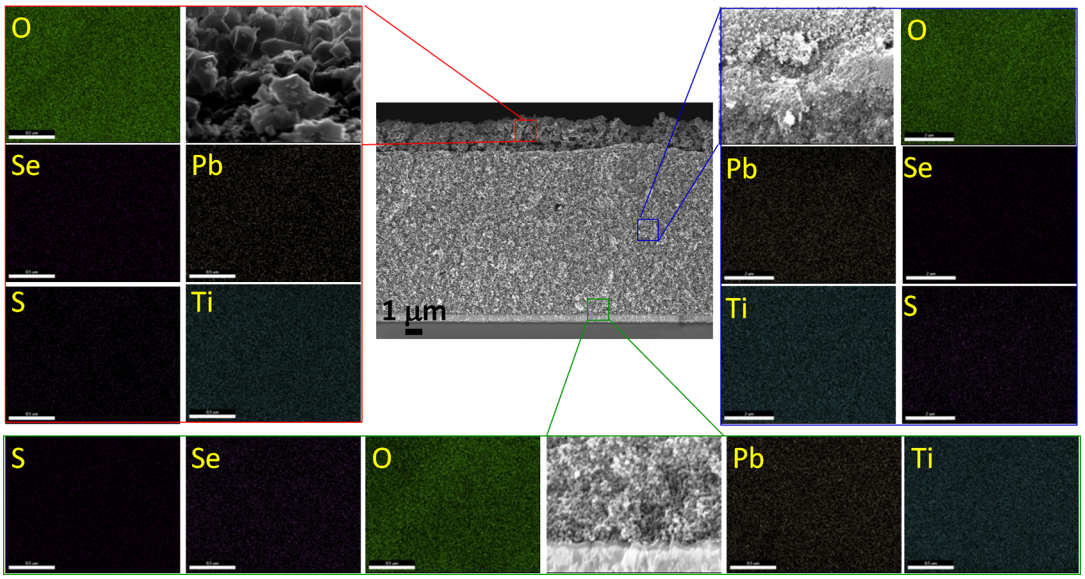

Figure 1. SEM analysis of a nanostructured TiO_2 sensitized with PbSeS QDs, t_d = 60 min. The central picture of a photoanode cross section is surrounded by a magnified image and elemental maps of the three square boxes in the central picture. Elemental maps display the Ti, O, Pb, Se, and S spatial elemental distribution.

more than one cell was prepared; standard errors were calculated for these conditions and are included in Tables 1 and 2. In a few cases just a single cell was analyzed; in those cases errors are not provided. IS measurements were carried out in the dark at different bias voltages with 10 mV AC perturbation over a frequency range of 400 kHz to 10 mHz.

RESULTS AND DISCUSSION

QDSCs have been prepared in this work by electrophoretic deposition of PbS and PbSeS QDs. It has been shown that PbSeS QDs offer certain benefits with respect to PbS or PbSe QDs in depleted heterojunction solar cells.[35] Figure 1 shows a cross section of a PbSeS-sensitized TiO_2 film prepared by EPD. The double layer structure of TiO_2 can be appreciated with a thicker TiO_2 transparent layer and a thinner top scattering layer. Elementary mapping of Ti, O, Se, S, and Pb at three different positions (i.e., sample depths) indicates that the deposition of colloidal PbSeS QDs was uniform along the TiO_2 thickness, ruling out a preferential deposition on the top layer. A rather continuous coating, with no inhomogeneities at the nanoscale level, is detected by comparing high-magnification scanning electron micrographs of samples before and after electrophoretic deposition (Figure S1, Supporting Information). It is worth mentioning that no effect of the electrophoretic deposition time, t_d, on the coating homogeneity was detected.

Solar cells prepared with photoanodes sensitized with PbS and PbSeS QDs show poor stability with polysulfide electrolyte. It has been shown that PbS is photocorroded in polysulfide electrolyte[23] and needs to be protected from direct contact with the electrolyte. This is accomplished in this work by coating a CdS layer, using the SILAR technique, on top of PbSeS and PbS QDs deposited by electrophoresis. CdS coating has been demonstrated previously to be an efficient protection of PbS, with a significant enhancement of the solar cell efficiency and stability.[29] In this sense, we have used a CdS coating, deposited by SILAR, to protect the PbSeS and PbS QDs from the corrosive effect of polysulfide electrolyte, obtaining stable devices.

For photoanode sensitization with PbSeS 800 nm, different deposition times t_d have been investigated. Hereafter, to distinguish among the different QD sizes analyzed after the QD type (PbS or PbSeS), we will add the wavelength of the first excitonic absorption peak. Figure 2a presents the absorption, in the allowed range of our experimental setup, of differently sensitized TiO_2 films: a bare TiO_2 film, a film sensitized just with five SILAR cycles of CdS, and a film sensitized with 800 nm PbSeS QDs plus five SILAR cycles of CdS at different deposition times. The absorption of the different samples has

dx.doi.org/10.1021/jp3056009 | J. Phys. Chem. C 2012, 116, 16391−16397

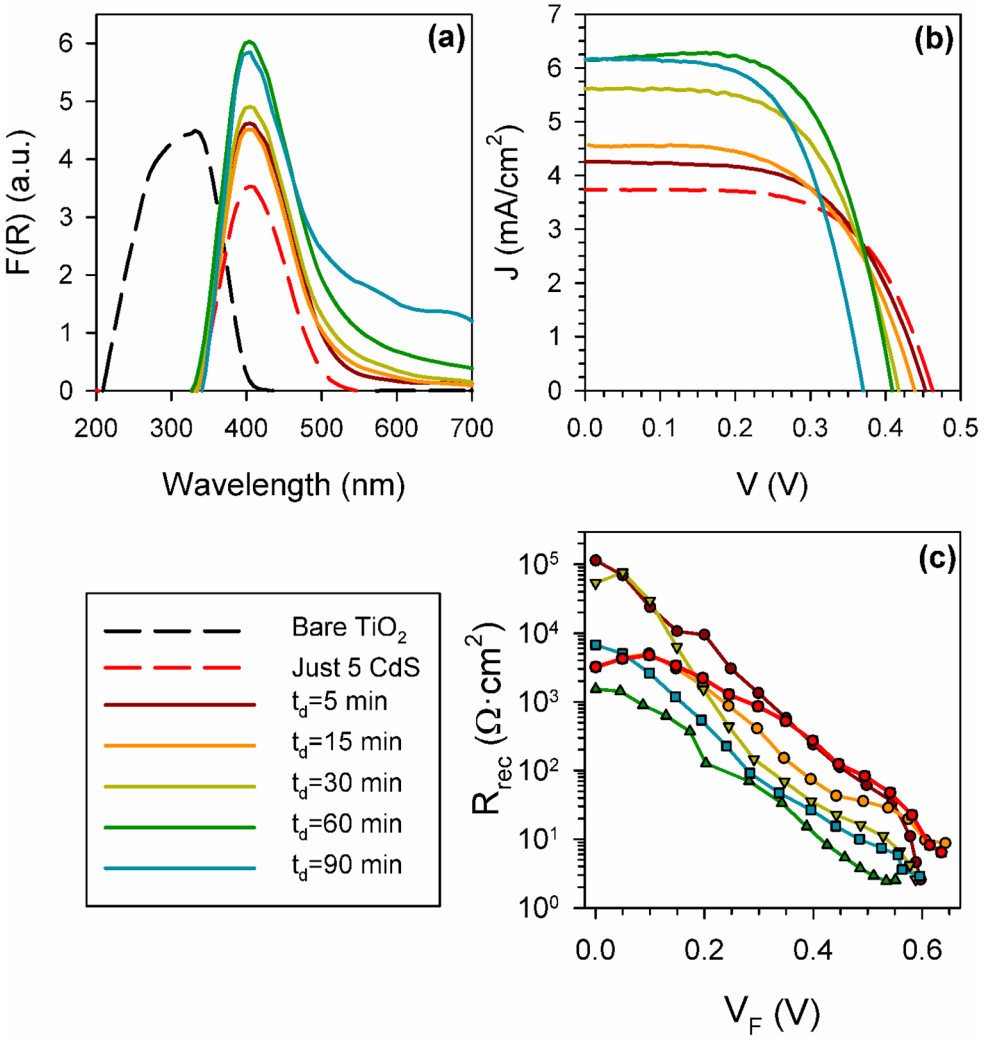

Figure 2. Effect of the electrophoretic deposition time, using 800 nm PbSeS QDs on (a) the Kubelka–Munk plot of the diffuse reflectance spectra for a bare TiO_2 film and TiO_2 sensitized just with five SILAR cycles of CdS and with 800 nm PbSeS QDs plus five SILAR cycles of CdS, (b) the J–V curve, and (c) the recombination resistance.

been extracted from their diffuse reflectance R and is expressed in Kubelka–Munk units as $F(R) = (1 - R)^2/2R$. For the sensitized electrodes the absorption of TiO_2 substrate has been removed. The film sensitized just with CdS exhibits an absorption threshold at 550 nm. When PbSeS QDs are deposited and coated with CdS, the absorption threshold red shifts, causing light absorption in the red visible region to increase due to a higher colloidal QD loading with deposition time.

Figure 2b shows the current–potential curves obtained for QDSCs using photoanodes with different t_d values; the solar cell parameters corresponding to these cells can be found in Table 1. When colloidal PbSeS QDs are deposited before CdS, the photocurrent of the cells increases due to the higher light harvesting capability provided by PbSeS QDs; see Figure 2a. However, this is associated with a decrease in the open circuit voltage, V_{oc}, as the QD loading increases. It should be expected that the ligands are preserved in the electrophoretic deposition, although the photoinjection is still possible. Efficient photoinjection has been previously reported for devices using colloidal QDs. CdSe QDs capped with TOP directly adsorbed on TiO_2 show a rather high APCE, ~90%,[36] and also colloidal QDS attached to TiO_2 using linker molecules present a significant photocurrent.[19,21,37]

The maximum performance in the analyzed cases has been obtained for t_d = 60 min. The origin of the decrease of V_{oc} can be understood by the analysis of impedance spectroscopy (EIS) data on the basis of the previously proposed models.[38,39] Samples with different deposition times present the same chemical capacitance, see the Supporting Information, section S2, indicating that the conduction band position and the density of states of TiO_2 are not affected by the QD loading. A clear trend in the recombination resistance is observed, Figure 2c. The recombination resistance is seen to decrease with t_d, indicating unambiguously that PbSeS QDs participate in the recombination process.[40] Recombination increases with the QD loading. PbSeS QDs act as recombination centers as has also been observed recently for Sb_2S_3.[41,42] The observation of this fact is decisive for the future optimization of the QDSCs. On the other hand, the reduction of recombination resistance due to an increase in QD loading produces the observed decrease in V_{oc}, which adversely affects on the solar cell performance; see Table 1. Note that both the PbSeS colloidal QDs and CdS coating contribute to the final light harvesting. PbSeS QDs are responsible for light absorption of wavelengths

dx.doi.org/10.1021/jp3056009 | J. Phys. Chem. C 2012, 116, 16391–16397

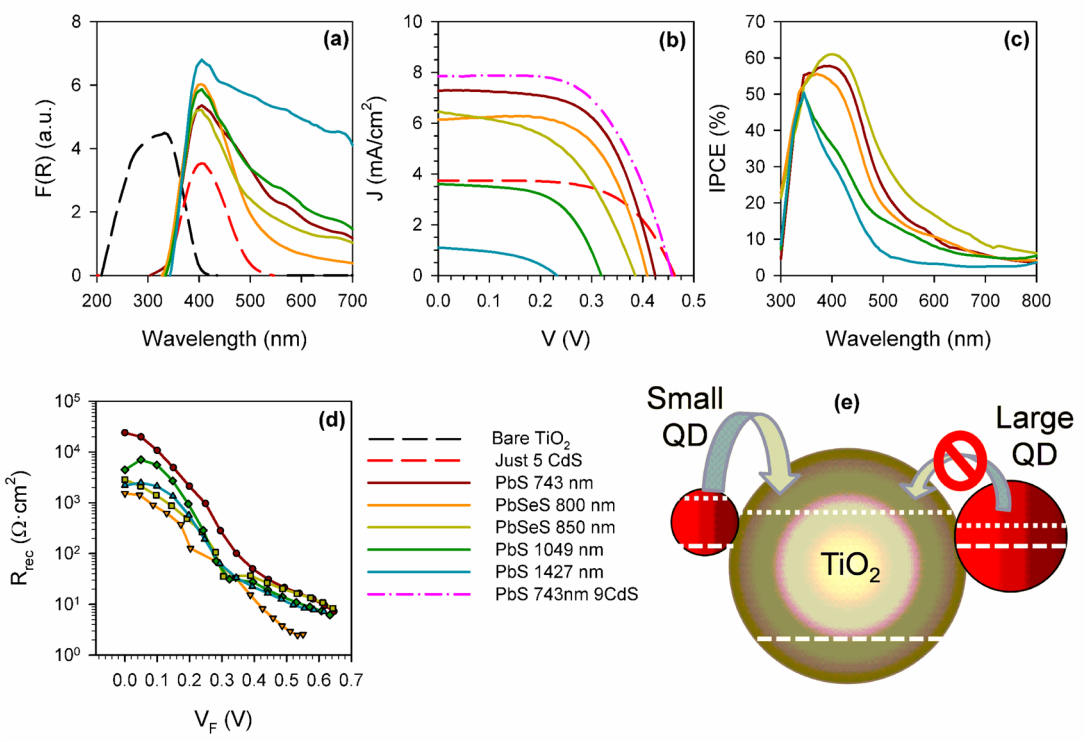

Figure 3. Effect of the QDs using the same electrophoretic deposition time, 60 min on (a) the Kubelka–Munk plot of the diffuse reflectance spectra for a bare TiO_2 film and TiO_2 sensitized just with five SILAR cycles of CdS and with 800 nm PbSeS QDs plus five SILAR cycles of CdS, (b) the J–V curve, (c) the IPCE, and (d) the recombination resistance. (e) Scheme of the relative alignment of the conduction band (dotted lines) of TiO_2 and PbS/PbSeS QDs depending on the QD size. Relative valence bands (dashed lines) are also included as a reference.

lower than ~550 nm, while for wavelengths higher than ~550 nm both PbSeS QDs and CdS contribute to the light absorption, but with a higher part from CdS; see Figure 2a.

We have also analyzed the effect of QD size in the final solar cell performance using PbSeS and PbS QDs of different sizes keeping t_d constant; see Figure 3. As the first excitonic absorption peak shifts to the IR region, the light absorption in the visible region increases, Figure 3a, but the increase in the light harvesting capability does not translate into greater efficiency of QDSCs or in an increase of the photocurrent, J_{sc}; see Figure 3b and Table 2. In fact, a systematic decrease of V_{oc} and J_{sc} is observed, with the highest efficiency obtained using PbS 743 nm QDs, i.e., the QDs with the smallest size (largest band gap). The relation between the wavelength of the first excitonic absorption peak and PbS QD size is described in the Supporting Information, section S3, using data from ref 43.

The decrease of solar cell performance with an increase of the size of the QDs has two causes. On one hand, the recombination resistance depends on the QD size; see Figure 3d. The sample with PbS 743 nm presents the highest recombination resistance (lowest recombination rate). On the other hand, there is an especially interesting discrepancy between light absorption and IPCE, Figure 3c. This discrepancy is clearly manifested for the biggest QDs, PbS 1427 nm. In this case, the sensitized photoanode presents strong light absorption in all the visible region, but practically null IPCE at wavelengths higher than 500 nm, indicating that PbS does not contribute to the photocurrent. In this case only the CdS light absorber contributes to the photocurrent, as can be observed from the IPCE measurements. This result is in good agreement with the work of Hyun et al.[43] In that work it has been shown that PbS QDs with size bigger than 4.3 nm (wavelength of the first excitonic absorption peak 1116 nm) cannot inject into the TiO_2 conduction band (CB) as its conduction band is lower than the CB of TiO_2, as indicated schematically in Figure 3e. As the QD size decreases, the band gap increases, shifting the PbS CB to higher energies than the TiO_2 CB, allowing electron injection from PbS with a small size into TiO_2. As the quantum confinement increases, the energetic distance between both CBs increases too, enhancing the injection driving force and consequently the photocurrent.

Having shown that the recombination pathway is preferentially through PbS QDs and also that it depends on the QDs size, recombination in this QDSC has to be related to QD traps. Note that, for PbS 1427 nm QDs, which do not inject electrons into TiO_2, the cell performance is significantly lower than for the cell just with five CdS SILAR cycles; see Figure 3b. This implies that the PbS QDs act as recombination centers in all the analyzed cases even when they are not able to inject photoexcited electrons into TiO_2. On the other hand, PbSeS QDs present lower recombination resistance than PbS, indicating a higher recombination rate than their PbS counterparts.

Additionally, for the QD size with the highest performance, PbS 743 nm, we have modified the number of CdS SILAR cycles, obtaining an efficiency as high as 2.1 ± 0.2% for nine SILAR cycles (1.8% for the sample just with nine SILAR cycles of CdS); see Figure 3b and Table 2. Significantly, this efficiency is very close to our previously reported efficiency of 2.21% for a PbS/CdS, both grown by SILAR and using the same TiO_2 electrode,[29] which conventionally produces solar cells with higher efficiencies than colloidal QDs.[44]

dx.doi.org/10.1021/jp3056009 | J. Phys. Chem. C 2012, 116, 16391–16397

CONCLUSIONS

In summary, we have sensitized nanostructured TiO_2 photoanodes with colloidal QDs of PbSeS and PbS with different sizes. We have shown that the electrophoretic deposition method can be used advantageously for fast sensitization of the photoanode with these QDs. CdS coating, deposited by SILAR, protects the colloidal QDs, stabilizing the solar cell performance. A clear effect between QD size and device performance is observed, obtaining better results for the smallest QDs, with efficiencies as high as 2.1 ± 0.2%. In addition, we have shown unambiguously that QDs act as recombination centers in these QDSCs. There is plenty of room for the optimization of these devices by focusing on reducing recombination through the QD traps. The latter may be possible by improving control of the QD properties; further characterization and surface treatments seem thus to be crucial. As an example, PbSeS-sensitized photoanodes were here characterized by X-ray diffraction, and the presence of a lead oxide (PbO) phase was detected, irrespectively of the t_d (Supporting Information, section S4). Although the origin of oxidation and its final effect on solar cell performance is currently under investigation, this finding points out the wide room of improvement of present lead chalcogenide QDSCs.

ASSOCIATED CONTENT

Supporting Information

FE-SEM micrographs of cross sections of TiO_2 and TiO_2/PbSSe samples, chemical capacitance of the analyzed cells, correlation between the PbS QD size and wavelength of the first excitonic absorption peak, and XRD characterization. This material is available free of charge via the Internet at http://pubs.acs.org.

AUTHOR INFORMATION

Corresponding Author

*E-mail: nima.parsibenehkohal@mail.mcgill.ca (P.B.); sero@fca.uji.es (I.M.-S.).

Notes

The authors declare no competing financial interest.

ACKNOWLEDGMENTS

This work was supported by the Institute of Nanotechnologies for Clean Energies, funded by the Generalitat Valenciana under Project ISIC/2012/008. This work was partially supported by the European Union under Project ORION CP-IP 229036-2, the Ministerio de Educación y Ciencia of Spain under Projects HOPE CSD2007-00007 (Consolider-Ingenio 2010) and JES-NANOSOLAR PLE2009-0042, the Generalitat Valenciana under Project PROMETEO/2009/058, an NSERC (Canada) strategic project grant, and a McGill University MEDA scholarship. R.T.-Z. acknowledges the support of the Program Ramón y Cajal of the MICINN. We acknowledge NANOCO for providing kindly PbSeS QDs.

REFERENCES

(1) Shockley, W.; Queisser, H. J. *J. Appl. Phys.* **1961**, *32*, 510−519.
(2) Nozik, A. J. *Physica E* **2002**, *14*, 115−200.
(3) Schaller, R. D.; Klimov, V. I. *Phys. Rev. Lett.* **2004**, *92*, 186601.
(4) Ellingson, R. J.; Beard, M. C.; Johnson, J. C.; Yu, P.; Micic, O. I.; Nozik, A. J.; Shabaev, A.; Efros, A. L. *Nano Lett.* **2005**, *5*, 865−871.
(5) Trinh, M. T.; Houtepen, A. J.; Schins, J. M.; Hanrath, T.; Piris, J.; Knulst, W.; Goossens, A. P. L. M.; Siebbeles, L. D. A. *Nano Lett.* **2008**, *8*, 1713−1718.
(6) Sambur, J. B.; Novet, T.; Parkinson, B. A. *Science* **2010**, *330*, 63−66.
(7) Semonin, O. E.; Luther, J. M.; Choi, S.; Chen, H.-Y.; Gao, J.; Nozik, A. J.; Beard, M. C. *Science* **2011**, *334*, 1530−1533.
(8) O' Regan, B.; Grätzel, M. *Nature* **1991**, *353*, 737−740.
(9) Grinis, L.; Dor, S.; Ofir, A.; Zaban, A. *J. Photochem. Photobiol., A* **2008**, *198*, 52−59.
(10) Mora-Seró, I.; Lana-Villarreal, T.; Bisquert, J.; Pitarch, A.; Gómez, R.; Salvador, P. *J. Phys. Chem. B* **2005**, *109*, 3371−3380.
(11) Islam, M. A.; Xia, Y.; Telesca, D. A., Jr.; Steigerwald, M. L.; Herman, I. P. *Chem. Mater.* **2004**, *16*, 49−54.
(12) Jia, S.; Banerjee, S.; Herman, I. P. *J. Phys. Chem. C* **2008**, *112*, 162−171.
(13) Islam, M. A.; Herman, I. P. *Appl. Phys. Lett.* **2002**, *80*, 3823−3825.
(14) Farrow, B.; Kamat, P. V. *J. Am. Chem. Soc.* **2009**, *131*, 11124−11131.
(15) Zhang, Q.; Xu, T.; Butterfield, D.; Misner, M. J.; Ryu, D. J.; Emrick, T.; Russell, T. P. *Nano Lett.* **2005**, *5*, 357−361.
(16) Brown, P.; Kamat, P. V. *J. Am. Chem. Soc.* **2008**, *130*, 8890−8891.
(17) Chen, J.; Lei, W.; Li, C.; Zhang, Y.; Cui, Y.; Wang, B.; Deng, W. *Phys. Chem. Chem. Phys.* **2011**, *13*, 13182−13184.
(18) Salant, A.; Shalom, M.; Hod, I.; Faust, A.; Zaban, A.; Banin, U. *ACS Nano* **2010**, *4*, 5962−5968.
(19) Giménez, S.; Mora-Seró, I.; Macor, L.; Guijarro, N.; Lana-Villarreal, T.; Gómez, R.; Diguna, L. J.; Shen, Q.; Toyoda, T.; Bisquert, J. *Nanotechnology* **2009**, *20*, 295204.
(20) Robel, I.; Subramanian, V.; Kuno, M.; Kamat, P. V. *J. Am. Chem. Soc.* **2006**, *128*, 2385−2393.
(21) Mora-Seró, I.; Giménez, S.; Fabregat-Santiago, F.; Gómez, R.; Shen, Q.; Toyoda, T.; Bisquert, J. *Acc. Chem. Res.* **2009**, *42*, 1848−1857.
(22) Hodes, G. *J. Phys. Chem. C* **2008**, *112*, 17778−17787.
(23) Lee, H. J.; Leventis, H. C.; Moon, S.-J.; Chen, P.; Ito, S.; Haque, S. A.; Torres, T.; Nüesch, F.; Geiger, T.; Zakeeruddin, S. M.; et al. *Adv. Funct. Mater.* **2009**, *19*, 2735−2742.
(24) Ma, B.; Wang, L.; Dong, H.; Gao, R.; Geng, Y.; Zhu, Y.; Qiu, Y. *Phys. Chem. Chem. Phys.* **2011**, *13*, 2656−2658.
(25) Snaith, H. J.; Stavrinadis, A.; Docampo, P.; Watt, A. A. W. *Sol. Energy* **2011**, *85*, 1283−1290.
(26) Acharya, K. P.; Khon, E.; O'Conner, T.; Nemitz, I.; Klinkova, A.; Khnayzer, R. S.; Anzenbacher, P.; Zamkov, M. *ACS Nano* **2011**, *5*, 4953−4964.
(27) Im, S. H.; Kim, H.-J.; Kim, S. W.; Kimb, S.-W.; Seok, S. I. *Energy Environ. Sci.* **2011**, *4*, 4181−4186.
(28) Lee, H. J.; Chen, P.; Moon, S.-J.; Sauvage, F.; Sivula, K.; Bessho, T.; Gamelin, D. R.; Comte, P.; Zakeeruddin, S. M.; Seok, S. I.; et al. *Langmuir* **2009**, *25*, 7602−7608.
(29) Braga, A.; Giménez, S.; Concina, I.; Vomiero, A.; Mora-Seró, I. *J. Phys. Chem. Lett.* **2011**, *2*, 454−460.
(30) Samadpour, M.; Boix, P. P.; Giménez, S.; Iraji Zad, A.; Taghavinia, N.; Mora-Seró, I.; Bisquert, J. *J. Phys. Chem. C* **2011**, *115*, 14400−14407.
(31) Hossain, M. A.; Koh, Z. Y.; Wang, Q. *Phys. Chem. Chem. Phys.* **2012**, *14*, 7367−7374.
(32) Zhou, N.; Chen, G.; Zhang, X.; Cheng, L.; Luo, Y.; Li, D.; Meng, Q. *Electrochem. Commun.* **2012**, *20*, 97−100.
(33) Kinder, E.; Moroz, P.; Diederich, G.; Johnson, A.; Kirsanova, M.; Nemchinov, A.; O'Connor, T.; Roth, D.; Zamkov, M. *J. Am. Chem. Soc.* **2011**, *133*, 20488−20499.
(34) Yang, Y.; Rodríguez-Córdoba, W.; Xiang, X.; Lian, T. *Nano Lett.* **2012**, *12*, 303−309.
(35) Ma, W.; Luther, J. M.; Zheng, H.; Wu, Y.; Alivisatos, A. P. *Nano Lett.* **2009**, *9*, 1699−1703.
(36) Giménez, S.; Xu, X.; Lana-Villarreal, T.; Gómez, R.; Agouram, S.; Muñoz-Sanjosé; Mora-Seró, I. *J. Appl. Phys.* **2010**, *108*, 064310.
(37) Watson, D. F. *J. Phys. Chem. Lett.* **2010**, *1*, 2299−2309.

(38) Fabregat-Santiago, F.; Garcia-Belmonte, G.; Mora-Seró, I.; Bisquert, J. *Phys. Chem. Chem. Phys.* **2011**, *13*, 9083−9118.
(39) Gónzalez-Pedro, V.; Xu, X.; Mora-Seró, I.; Bisquert, J. *ACS Nano* **2010**, *4*, 5783−5790.
(40) Hod, V.; González-Pedro, Z.; Tachan, F.; Fabregat-Santiago, I.; Mora-Seró, J.; Bisquert; Zaban, A. *J. Phys. Chem. Lett.* **2011**, *2*, 3032−3035.
(41) Boix, P. P.; Larramona, G.; Jacob, A.; Delatouche, B.; Mora-Seró, I.; Bisquert, J. *J. Phys. Chem. C* **2012**, *116*, 1579−1587.
(42) Boix, P. P.; Lee, Y. H.; Fabregat-Santiago, F.; Im, S. H.; Mora-Seró, I.; Bisquert, J.; Seok, S. I. *ACS Nano* **2012**, *6*, 873−880.
(43) Hyun, B.-R.; Zhong, Y.-W.; Bartnik, A. C.; Sun, L.; Abruña, H. D.; Wise, F. W.; Goodreau, J. D.; Matthews, J. R.; Leslie, T. M.; Borrelli, N. F. *ACS Nano* **2008**, *2*, 2206−2212.
(44) Guijarro, N.; Lana-Villarreal, T.; Shen, Q.; Toyoda, T.; Gómez, R. *J. Phys. Chem. C* **2010**, *114*, 21928−21937.